On-Water Radiometry Measurements: Skylight-Blocked Approach and Data Processing

Zhongping Lee [1], Jianwei Wei [1], Zhehai Shang [1], Rodrigo Garcia [1], Heidi Dierssen [2], Joji Ishizaka [3], Alexandre Castagna [4]

[1] University of Massachusetts Boston, Boston, Massachusetts 02125, USA

[2] University of Connecticut, Connecticut, 06340 USA

[3] Institute for Space-Earth Environmental Research, Nagoya University, Japan

[4] Protistology and Aquatic Ecology, Gent University, Krijgslaan 281, Gent 9000, Belgium

1. INTRODUCTION

The in-water and above-water approaches discussed in Zibordi et al. (2019) derive, rather than directly measure, the water-leaving radiance (L_w). In addition to these "standard" approaches, there exists a scheme that directly measures L_w for the calculation of the remote sensing reflectance (R_{rs}). This scheme attaches an open-ended apparatus (either cone- or dome-shaped or cylindrical) to the front of a downward-looking radiance radiometer. This apparatus penetrates a few centimeters through the water's surface, while keeping the radiometer in air. This setup effectively blocks the skylight (used as a generic term here, including sunlight) from illuminating the water surface within the field-of-view of the radiometer, and blocks surface-reflected light (from both sky and the sun) from entering the field-of-view of the radiometer, so allows for a direct measurement of L_w. Ahn (1999) demonstrated this approach of measuring L_w, followed by Tanaka et al. (2006) who tested a dome-cover apparatus to carry out L_w measurements. Lee et al. (2010), Kutser et al. (2016; 2013) and Castagna (2019) further experimented with a tube that blocked surface-reflected light. More recently, Lee et al. (2013) configured a dynamic and durable system using commercially available radiometers and thoroughly investigated this measurement scheme, which was subsequently termed the "skylight-blocked approach (SBA)" for the direct measurement of water-leaving radiance. Compared to the standard in-water and above-water approaches, the SBA can be classified as "on-water radiometry", but importantly it incorporates an apparatus that blocks both surface-reflected light and skylight from reaching the surface under view measurement (Figure 1). This approach has the following unique features compared to the in-water and above-water measurement schemes, whereby:

1) It measures L_w directly; avoiding post-processing procedures such as the extrapolation of $L_u(z)$ to $L_u(0^-)$ required for the in-water approach, or the removal of surface-reflected light required for the above-water approach.

2) It is applicable to all aquatic environments, whereas the in-water approach is challenging to deploy when the bottom depth is shallow or when strong near-surface stratification causes large uncertainties in the extrapolation of $L_u(z)$ to $L_u(0^-)$.

3) It accurately derives the R_{rs} under variable sky conditions, unlike the above-water approach which will generate large uncertainties if there are scattered, moving clouds (even when the Sun is not blocked), or in inland waters (e.g., pond, narrow river or inlet) where diffuse skylight is not easily characterized due to adjacent vegetation or structures.

Similar to in-water radiometry, the SBA measurements are subject to errors due to instrument self-shading. To correct these errors, Shang et al. (2017) developed a correction scheme for processing SBA data based on spectral optimization, and this scheme can be adapted for different deployment platforms. The ideal solution for reducing the self-shading effect is to use an apparatus with a very small diameter (<1 cm for most aquatic environment and for the

~350 – 800 nm spectral range). To date, the SBA scheme for L_w (and R_{rs}) has been tested in shallow, coastal, and oceanic waters and inland waters with high performance (Castagna et al. 2019; Kutser et al. 2016; Kutser et al. 2013; Lee et al. 2013; Wei et al. 2018; Wei et al. 2015).

An accurate determination of the remote sensing reflectance (R_{rs}) requires the ambient light for L_w and the downwelling irradiance (E_s) be the same, which can be achieved by measuring both L_w and E_s simultaneously, or limiting the measurements when the ambient light is stable. For simultaneous measurements to ensures the "same" illumination conditions for both L_w and E_s, two calibrated radiometers are recommended and adopted for SBA (as the commonly adopted simultaneous measurements of the in-water approach). The final products from SBA generally include spectra of the R_{rs} and the standard deviation (STD). We here describe the instrument configuration, measurement and data processing procedures related to SBA with such a setup. Separately, Olszewski and Sokolski (1990) proposed a contactless skylight-blocking scheme to screen out surface reflected contributions while taking radiance measurements of water from above the surface, but its measurement methods and discussion are not included here.

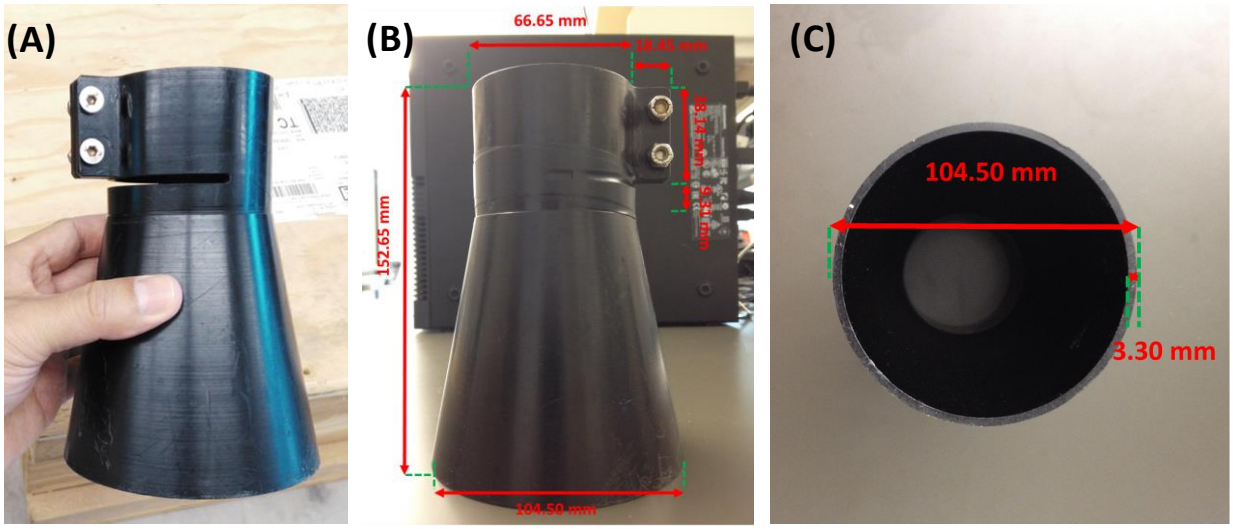

Figure 1. Dimensions of a cone-shaped prototype skylight-blocking apparatus. Note that the dimensions are subject to specifications of the downward looking radiometer.

2. MEASUREMENTS

Skylight-blocking apparatus

A rule of thumb for the design of the skylight-blocking apparatus is to ensure that it should maximize the measurement performance. First, this apparatus should not be bulky, as self-shading error is proportional to size. Second, it is important to avoid interference with the FOV of the radiometer (here defined as the full angle of view), as it will complicate the radiometric calibration. Third, it should be fabricated in a dark matte color to minimize the light reflection off its own surface. Finally, the apparatus should be weather resistant. An example (see Figure 1) of such an apparatus was made in the shape of a cone and manufactured from Black Acetron. The cone, illustrated in Figure 1 has a bottom diameter of 104.50 mm, a parallel cross section on the upper side of 66.65 mm in diameter and 105.2 mm in height. The uppermost part of the apparatus is a cylindrical collar attachable to a radiometer. The apparatus shown here was specifically manufactured for commercial radiometers with a FOV of 23° in air. For other radiometers with different specification, it is advised to adjust the dimension for the cone or cylinder accordingly. The following formula can be used to calculate the opening of the skylight-blocking apparatus to define its minimum diameter (Y):

$$Y \geq D + 2 \times X \times \tan(\mathrm{FOV}/2), \quad (1)$$

where X is the distance from the lens to the opening of the skylight-blocking apparatus and D is the effective diameter of the lens.

Instrument configuration

In the deployment, the downward-looking radiometer with the SBA should be maintained in air such that it receives the light emerging from the water in a specified direction (so far it is commonly in the nadir direction). The base of the cone should be beneath the water surface, while the fore optics of the radiometer located in air. With such a setup, light from the sky illuminating the viewing area and light reflected by the sea surface are blocked by the cone, while only the radiance emerging from beneath the water surface will be measured. A configuration for the various components for the L_w measurement is shown in Figure 2. In this example, the radiometer for downwelling irradiance counter-balances the radiance sensor with a balanced flotation collar, so that L_w and E_s of the "same" place are recorded contemporaneously. Figure 2 provides an example of such a measurement system that is easy to handle, strong enough to hold the sensors, and small enough to minimize the impact on the ambient light field. Other deployment strategies, such the handheld approach (e.g., Lee et al. 2010; Kuster et al. 2013, 2016; Castagna et al. 2019), are certainly also options, although likely different uncertainties could be involved and should be evaluated for accurate determination of L_w (or R_{rs}). The following rather focuses on the deployment strategy showing in Figure 2.

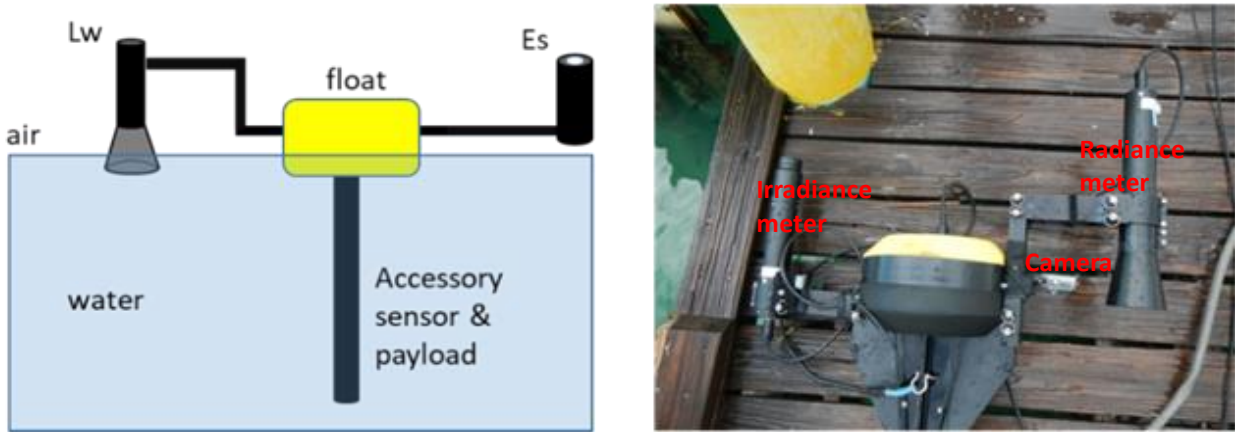

Figure 2. Design and configuration of a prototype radiometric package equipped with SBA. A sonar component for bottom depth is outside of the picture.

Avoidance or minimization of perturbations during deployment

As with in-water and above-water radiometric measurements, perturbations (including those from the float and the upper structure of the ship) to the measurement of L_w and E_s should be avoided or minimized during the deployment of the system. For the setup showing in Figure 2, where radiance and irradiance are measured on the water, the instrument package should be kept away from the operating ship to minimize reflection and shadowing from the ship. Based on Monte Carlo simulations, we recommend that an SBA system similar to Figure 2 should be in general kept at a distance of 3 times the height of the operating ship (i.e. ~30 m if ship's height is 10 m) to keep ship-induced uncertainty less than 1% (Shang et al. in review). On a slow-moving vessel, it is recommended to use caution to avoid white-wash and ship wakes. Specific to the L_w measurements and a configuration similar to Figure 2, it is strongly recommended that the orientation of the instrument be maintained with the SBA radiance sensor facing the Sun (e.g. ±45° from the solar plane) to minimize potential shadowing effect from the float. Such an orientation may be achieved by interchanging the radiance and irradiance radiometers according to the Sun's position, water current and wind directions. For example, if the radiance sensor is faced towards the Sun in the morning, it might be necessary to

interchange it with irradiance sensor for similar illumination geometry in the afternoon. To minimize the shadowing effects from the float, an extension arm is recommended to keep the radiance sensor away from the central float. As shown in Figure 2, the arms are about 30 cm in length.

Radiometric calibration and characterization

Both radiometers for radiance and irradiance measurements should be calibrated with national measurement institute standards. Radiometer's calibration and characterization should be performed following state-of-the-art methods, with an uncertainty of ~1% or less. The calibration and characterization should take into account the stray light correction, linearity, polarization sensitivity, etc. (see Chapter 3 of this protocol). As the radiometer fore optics are not expected to be immersed in the water, an immersion factor is not required. The radiometer for irradiance measurement should be calibrated (better to be designed) for measurement in air.

Dark signal

Dark signals should be measured periodically to obtain dark current measurements. This is straightforward if the radiometers are capable of closing an onboard shutter over the spectrometer before sensor sampling and telemetry output. Alternatively, when no onboard shutters are available, it can also be performed by closing the fore optics with a cap and then taking measurements.

Ancillary data and metadata

Observation time, latitude and longitude coordinates, wind speed, sea state, and instrument tilt are important information for each measurement, although not all will be used for the post-processing of radiometric measurements. Other ancillary information, including water temperature and salinity, is also recommended to facilitate data analysis. Also, for the configuration given in Figure 2, it is recommended to record meta-data related to the orientation of the sensor with respect to the sun, as it can be informative for assessing the uncertainty due to shading effects.

For optically shallow waters, it is useful to attach a submersible camera (see Figure 2) to the float to identify the benthic substrate associated with the reflectance spectra, as well as a sonar component to get the co-registered bottom depth.

Time span for measurements

At each station, a time series (e.g., 5-10 minutes) of continuous measurements of both radiance and irradiance are recorded (for a setup like that in Figure 2). This time span usually results in ~500 or more of radiance and irradiance spectra. For field measurement of R_{rs}, there is no intention or assumption that each of these scans is valid. Rather, we will select ~20-50 high-quality spectra for the calculation of final R_{rs} spectrum for the targeted site.

3. DATA ANALYSIS

Data preprocessing

The raw data from both sensors are converted to radiometric units by applying the calibration coefficients and dark current correction. The data are first interpolated onto a common time coordinate. The radiance and irradiance spectra are then interpolated to the same spectral resolution. The instantaneous remote sensing reflectance at time t, $R_{rs}(\lambda, t)$, can be determined from the ratio of the instantaneous $L_w(\lambda,t)$ to the corresponding $E_s(\lambda,t)$:

$$R_{rs}(\lambda,t) = \frac{L_w(\lambda,t)}{E_s(\lambda,t)} \tag{2}$$

Quality control

To ensure that only high-quality data are collected and used, we check for the instrument tilt and only keep those with low inclination. This avoids apparent Sun zenith cosine changes to the cosine collector of the E_s sensor that can

cause large bias. For a system with a single axis inclinometer, only data with tilt ≤ 5° should be used for further analysis (for E_s and nadir-viewing water-leaving radiance). However, it is noted that even with a 5° tilt of the sensor, errors can be large (up to ±20% error) if the relative azimuth of the tilt is close to the plane of the Sun (< ±45° or > ±135°) (Castagna et al. 2019), therefore the threshold for tilt angle could be set even smaller to reduce this uncertainty. A dual axis inclinometer is recommended for better quality control, with recorded system orientation (radiance sensor oriented to the Sun). In the field, prevailing winds, strong currents, waves, white-wash and choppy swell can cause the radiance sensor along with the cone of the SBA system either to pop out of the water surface or to submerge the fore optics of the radiometer into water. As a consequence, raw $L_w(t)$ (and $R_{rs}(t)$) require additional filtering described below:

1) The probability density function (PDF) will be calculated for $R_{rs}(\sim 698,t)$ (longer wavelengths are required for optically shallow waters) from the ~500 or more measurements. The first mode of the $R_{rs}(698,t)$ distribution is then located from the PDF.

2) All $R_{rs}(t)$ spectra with $R_{rs}(698,t)$ beyond ±15% of this mode are filtered out.

3) The remaining $R_{rs}(t)$ spectra are considered as the desired high-quality data and used to calculate average and standard-deviation spectra, as in Olszewski and Kowalczek (2000).

The rational for the above filtering procedure is that:

a) for longer wavelengths, water molecules have strong absorption, resulting in very low R_{rs} that may be close to 0, thus an enhancement in the R_{rs} in the longer wavelengths (for oceanic waters and most coastal waters) will most likely be the result of surface-reflected light, if the cone swings out of the surface due to swell;

b) "true" R_{rs} of a water body has a specific value, but contributions from surface-reflection or from submersion of the radiance sensor into water are random.

Self-shade correction

The self-shading error can be quantified with the algorithm of Shang et al. (2017). This algorithm only requires the solar zenith angle (θ_s), diameter of the cone (Y), and the R_{rs} spectrum obtained in Step 3 listed above (represented as R_{rs}^{shade} here). The basic workflow of the optimization scheme is referred to the spectral optimization method detailed in Lee et al. (1999). First, an R_{rs} spectrum free of shading error ($R_{rs}^{noshade}$) can be modeled as a function of absorption (a) and backscattering (b_b) coefficients (Gordon et al. 1988; Morel and Gentili 1993):

$$R_{rs}^{noshade}(\lambda) = f_1(a(\lambda), b_b(\lambda)). \tag{3}$$

Further, R_{rs}^{shade} is related to $R_{rs}^{noshade}$ as,

$$R_{rs}^{shade}(\lambda) = R_{rs}^{noshade}(\lambda) \times [1 - \varepsilon(\lambda)] \tag{4}$$

where ε is the shading error. Based on Monte Carlo (MC) simulations for the deployment system showing in Figure 2, ε is a function of a, b_b, Y and θ_s (Shang et al. 2017),

$$\varepsilon(\lambda) = f_2(a(\lambda), b_b(\lambda), Y, \theta_s) \tag{5}$$

Combining with Eq. (3)-(5) yields:

$$R_{rs}^{shade}(\lambda) = f_3(a(\lambda), b_b(\lambda), Y, \theta_s) \tag{6}$$

Using a spectral optimization procedure, a and b_b can be derived by matching the modeled R_{rs}^{shade} with the measured R_{rs}^{shade}. With known Y, θ_s and derived a&b_b, ε can be calculated following Eq. (5). Further, we get:

$$R_{rs}^{true}(\lambda) = \frac{R_{rs}^{shade}(\lambda)}{1 - \varepsilon(\lambda)} \tag{7}$$

Here, R_{rs}^{true} is the shade-corrected R_{rs} spectrum that is reported for each station. Based on MC simulations, the shading correction algorithm can reduce the measurement errors to < 2% in the visible domain from oceanic to turbid waters (Shang et al. 2017). A processing software following the above description is developed and available for download.

Quality assurance

Quality assurance (QA) should be carried out for each R_{rs} spectrum, and a scheme has been developed to assure the quality of an R_{rs} spectrum. The QA score system (Wei et al. 2016) is based on the water classification of the R_{rs} spectral shapes. The spectral shape of R_{rs} is represented by the normalized R_{rs} spectrum,

$$nR_{rs}(\lambda_i) = \frac{R_{rs}(\lambda_i)}{\left[\sum_{j=1}^{n} R_{rs}(\lambda_j)^2\right]^{1/2}},\ i = 1, 2, ..., n \tag{8}$$

where n refers to the number of spectral bands. This system classifies the R_{rs} spectra into predefined optical water types, and then calculate a QA score for each individual R_{rs} spectrum. The QA scores varies from 0 to 1, with 0 referring to the lowest quality and 1 the highest quality. Note that this system should not be the only way to measure the quality of an R_{rs} spectrum. Comparisons with measurements from other approaches as well as from modeling based on measured IOPs could also be considered. An alternative QA is to check if the R_{rs} in the near-infrared (NIR) matches the NIR water similarity spectrum if the waters are turbid (Ruddick et al. 2006; Sterckx et al. 2011), which may also detect under- or over-correction for shadowing effects.

Uncertainty in R_{rs}

The uncertainty in R_{rs} originates from environmental disturbances including clouds, waves, wave focusing, data reduction procedure (data filtering, mode determination, shade correction), sensor's calibration, etc. Water splashes can occur with system inclination and lenses should be checked at the end of deployment for quality control to reduce errors. The uncertainties of measured R_{rs} can be evaluated as the standard deviation, or the coefficient of variation (CV, ratio of standard deviation to mean), of the ensemble R_{rs} spectra. Two sample R_{rs} spectra are presented in Figure 3. One spectrum was obtained from the south Yellow Sea and the other measured at the Marine Optical Buoy (MOBY) site, east of Lanai, Hawaii. Also included is the spectrum of CV, where values of CV are less than ~6% for these examples. Especially, the CV values are ~3% for blue water at blue wavelengths, which are well below the targeted 5% for ocean waters at blue bands.

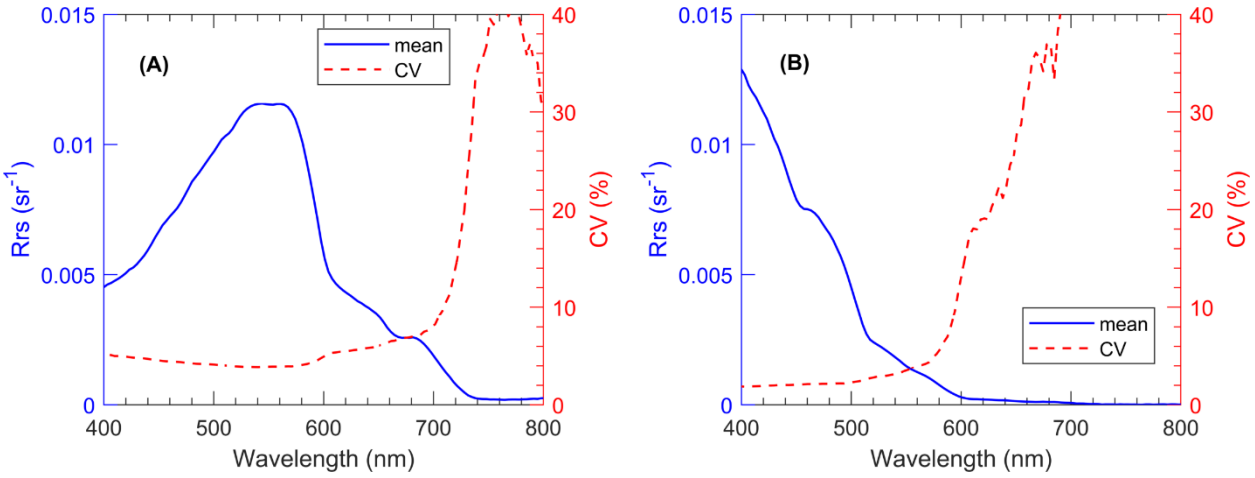

Figure 3. Examples of SBA-measured remote sensing reflectance spectra from (a) the South Yellow Sea and (b) the Marine Optical Buoy (MOBY) site.

4. VARIATIONS, RECOMMENDATIONS AND FUTURE DIRECTIONS

For the configuration given in Figure 2, there is likely a larger shading impact under high solar zenith angles and if the radiance sensor is oriented away from the Sun. This kind of error or uncertainty could be avoided or minimized by

different configurations, such as placing the radiance radiometer in the middle, rather than on one side of a float. Also, the skylight-blocking apparatus should be customized with respect to the radiometers in use. The critical factors to consider include the radiometer dimensions and sensor's field of view.

The radiometer for E_s can be placed on the superstructure of an operating ship, as long as there is an assurance that the E_s value measured is representative of the E_s value at the location where the radiance radiometer is located and no heating impact due to exposure in air. For E_s radiometers positioned similar to that in Figure 2, it is important to keep the cosine collector for E_s above any protrusions on the float system. The largest error source for SBA measurements of water-leaving radiance is self-shading, which is a function of the water's optical properties, sun elevation, and the size of the skylight-blocking cone and deployment platform. Among these four, the cone and platform size are the only parameters that can be determined at the designing/manufacturing phase of this system. Hence, it is highly desired to manufacture small-size radiometers that can be held by small platforms and incorporate a cone as small as possible. In high seas, it is recommended that the integration time of the radiance sensor be short to avoid contamination by surface-reflected light with movement of the cone.

The above-water skylight blocking scheme used by Olszewski and Sokolski (1990) requires both superfast data collection (in ms or less) and very small coverage area (in cm^2 or less). This scheme has not been widely known or tested. With the advancement of optical-electronic components/systems, it is worth evaluating this above-water SBA and comparing the results from the on-water SBA, as it may provide high-quality R_{rs} while an operation ship is underway.

REFERENCES

Ahn, Y.-H. (1999). Development of redtide & water turbidity algorithms using ocean color satellite. In (p. 287). Seoul, Korea: KORDI

Castagna, A., Simis, S., Dierssen, H., Vanhellemont, Q., Sabbe, K., & Vyverman, W. (2019). Extending Landsat 8: Retrieval of an orange contra-band for inland water quality applications. . *Rem. Sens.*, In review

Gordon, H.R., Brown, O.B., Evans, R.H., Brown, J.W., Smith, R.C., Baker, K.S., & Clark, D.K. (1988). A semianalytic radiance model of ocean color. *J. Geophys. Res., 93*, 10,909-910,924

Kutser, T., Paavel, B., Verpoorter, C., Ligi, M., Soomets, T., Toming, K., & Casal, G. (2016). Remote Sensing of Black Lakes and Using 810 nm Reflectance Peak for RetrievingWater Quality Parameters of Optically Complex Waters. *Rem. Sens., 8*, 497; doi:410.3390/rs8060497

Kutser, T., Vahtmäe, E., Paavel, B., & Kauer, T. (2013). Removing glint effects from field radiometry data measured in optically complex coastal and inland waters. *Rem. Sens. Envi., 133*, 85-89

Lee, Z.-P., Ahn, Y.-H., Mobley, C., & Arnone, R. (2010). Removal of surface-reflected light for the measurement of remote-sensing reflectance from an above-surface platform. *Optics Express, 18*, 26313-26342

Lee, Z.-P., Pahlevan, N., Ahn, Y.-H., Greb, S., & O'Donnell, D. (2013). A robust approach to directly measure water-leaving radiance in the field. *Applied Optics, 52* 1693-1701

Lee, Z.P., Carder, K.L., Mobley, C.D., Steward, R.G., & Patch, J.S. (1999). Hyperspectral remote sensing for shallow waters: 2. Deriving bottom depths and water properties by optimization. *Applied Optics, 38*, 3831-3843

Morel, A., & Gentili, B. (1993). Diffuse reflectance of oceanic waters (2): Bi-directional aspects. *Applied Optics, 32*, 6864-6879

Olszewski, J., & Kowalczek, P. (2000). Sky glint correction in measurements of upward radiance above the sea surface. *Oceanologia, 42*, 251-262

Olszewski, J., & Sokolski, M. (1990). Elimination of the surface background in contactless sea investigations. *Oceanologia, 29*, 213-221

Ruddick, K.G., Cauwer, V.D., Park, Y.-J., & Moore, G. (2006). Seaborne measurements of near infrared water-leaving reflectance: The similarity spectrum for turbid waters. *Limnology and Oceanography, 51*, 1167-1179. DOI: 1110.4319/lo.2006.1151.1162.1167

Shang, Z., Lee, Z., Dong, Q., & Wei, J. (2017). Self-shading associated with a skylight-blocked approach system for the measurement of water-leaving radiance and its correction. *Applied Optics, 56*, 7033-7040

Shang, Z., Lee, Z.P., Wei, J., & Lin, G. (in review). Impact of ship on radiometric measurements in the field: A reappraisal via Monte Carlo simulations

Sterckx, S., Knaeps, E., & Ruddick, K.G. (2011). Detection and correction of adjacency effects in hyperspectral airborne data of coastal and inland waters: The use of the near infrared similarity spectrum. *International Journal of Remote Sensing, 32*, 6479-6505. DOI: 6410.1080/01431161.01432010.01512930

Tanaka, A., Sasaki, H., & Ishizaka, J. (2006). Alternative measuring method for water-leaving radiance using a radiance sensor with a domed cover. *Optics Express, 14*, 3099-3105

Wei, J., Lee, Z.-P., & Shang, S. (2016). A system to measure the data quality of spectral remote sensing reflectance of aquatic environments. *J. Geophys. R., 121*, 8189–8207

Wei, J., Lee, Z.P., Garcia, R., Zoffoli, M.L., Armstrong, R., Shang, Z., Sheldon, P., & Chen, R.F. (2018). An assessment of Landsat-8 atmospheric correction schemes and remote sensing reflectance products in coral reefs and coastal turbid waters. *Remote Sensing of Environment, 215*, 18-32

Wei, J., Lee, Z.P., Lewis, M., Pahlevan, N., Ondrusek, M., & Armstrong, R. (2015). Radiance transmittance measured at the ocean surface. *Optics Express, 23*, 11826-11837

Zibordi, G., Voss, K.J., Johnson, B.C. and Mueller, J.L. (2019). Protocols for Satellite Ocean Color Data Validation: In situ Optical Radiometry, IOCCG Ocean Optics and Biogeochemistry Protocols for Satellite Ocean Colour Sensor Validation, Volume 3, IOCCG, Dartmouth, NS, Canada.